SPECTRAL STUDIES OF IRON COORDINATION IN HEMEPROTEIN COMPLEXES: DIFFERENCE SPECTROSCOPY BELOW 250 mμ

ARTHUR S. BRILL *and* HOWARD E. SANDBERG

From the Department of Molecular Biophysics, Yale University, New Haven, Connecticut 06520. Dr. Sandberg's present address is the Department of Biochemistry and Biophysics, University of Hawaii, Honolulu, Hawaii 96822. Professor Brill's address after July 1 will be the Department of Materials Science, University of Virginia, Charlottesville, Virginia, 22901.

ABSTRACT In order to evaluate the feasibility of observing the spectral behavior of protein groups in the coordination sphere of the iron in hemeproteins, criteria are developed to determine whether or not the application of difference absorption spectroscopy to the study of complex formation will be successful. Absolute absorption spectra, 300–1100 mμ, from bacterial catalase complexes are displayed, and the infrared bands correlated with magnetic susceptibility values of similar complexes of other hemeproteins. Dissociation constants for the formation of cyanide and azide complexes of metmyoglobin, methemoglobin, bacterial catalase, and horseradish peroxidase are given. Difference spectra, 210–280 mμ, are displayed for cyanide and azide complexes of these hemeproteins. A band at 235–241 mμ is found in the difference spectra of all low-spin vs. high-spin complexes. The factors which favor the assignment of this band to a transition involving a histidine residue are presented.

INTRODUCTION

The special properties of metalloproteins as compared with other metal compounds depend, at least in part, upon the nature of the involvement of protein groups in the coordination sphere of the metal ion. A complete structure determination from single protein crystal X-ray diffraction data provides the micromorphology necessary to identify ligands. For metal ions with unpaired electrons, electron paramagnetic resonance can, in many cases, provide direct evidence for bound nitrogen atoms. Other kinds of measurement (e.g. hydrogen ion titration) suggest indirectly the participation of particular amino acid residues in bonds to metal, the residues being identified by some particular property (e.g. pK of an ionizing group, reactivity toward a blocking reagent). Experiments reported earlier (Brill and Sandberg, 1967) and here in greater detail offer the possibility that absorption spectrophotometry may be used to identify the protein groups which serve as ligands.

The characteristic absorption bands of the amino acid residues of protein fall below 300 mμ (Edsall, 1963). Down to 250 mμ, the total absorption by the aromatic side chains of tyrosine, tryptophan, and phenylalanine is usually not so great as to preclude observation of changes in any one residue by *absolute* spectrophotometry. Below 250 mμ, absorption by these three residues is joined by that from histidine, methionine, cystine, cysteine, and by the peptide bond which has a maximum in absorptivity at 190 mμ. All proteins show a sharp increase in total absorbance below 240 mμ, and the detection of small changes in the absolute spectra is rendered difficult. However, difference spectroscopy can be used to discriminate against contributions from residues which are electronically unperturbed while effects involving a particular group or groups are studied. In the case of hemeproteins, the latter groups are ones which contribute atoms at positions 5 and/or 6 of the coordination sphere of iron in heme (pyrrole nitrogens occupy positions 1 though 4). The principle of spectrophotometric isolation of amino acid chromophores has, of course, many more applications than the one to be given in this paper (Herskovits and Laskowski, 1962; Theorell and Yonetani, 1964; Fisher and Cross, 1965).

The kinds of chemical and physical changes which are to be dealt with can be illustrated by the behavior of ferrimyoglobin. The three-dimensional structure of his protein in several forms is known from the X-ray diffraction analyses of Kendrew and his colleagues. In acid ferrimyoglobin, the nitrogen of a histidine (imidazole group) is in position 5 and a water molecule, oxygen in position 6, is sandwiched between the iron atom and a distal histidine (Kendrew, 1962, 1963). Magnetic susceptibility measurements have shown that the iron is in the high-spin ($\frac{5}{2}$) state (Theorell and Ehrenberg, 1951; Scheler, Schoffa, and Jung, 1957), which is to say that all of the metal valence (3*d*) electrons are unpaired and the five iron-nitrogen bonds and one iron-oxygen bond are essentially ionic. When, for example, the azide complex is formed, the water molecule contributing to position 6 is displaced by the new ligand, an iron-nitrogen bond replacing the iron-oxygen bond (Stryer, Kendrew, and Watson, 1964). While the protein structure is unaffected at the resolution of the X-ray analysis, the electronic structure of the entire coordination sphere is known to have changed through observations which depend upon energy level differences. The position of the Soret band has shifted from 408 to 420 mμ (Scheler, Schoffa, and Jung, 1957). There are marked differences in the visible spectrum, the magnetic susceptibility has dropped to a value which corresponds more closely to that of the low-spin ($\frac{1}{2}$) state (one unpaired electron) than to the high, and the electron paramagnetic resonance spectrum has changed from axial to rhombic with all three *g*-values now in the region of the free electron value (Gibson and Ingram, 1957). The replacement of a water oxygen by an azide nitrogen at position 6 is seen to affect the coordination at the other five positions, all the metal-nitrogen bonds now being largely covalent. One may ask whether or not the shift to iron-

ligand molecular orbitals of electrons from the imidazole at position 5 produces a spectrophotometrically detectable change in the histidine residue.[1]

We report here measurements in the wavelength region 250–210 mμ which reveal bands in the difference spectra of low-spin complexes of respiratory pigments and heme enzymes vs. the free high-spin hemeproteins.

INSTRUMENTAL AND CHEMICAL CONSIDERATIONS

A Cary Model 14 recording spectrophotometer (Cary Instruments, Monrovia, Calif.) was used throughout these studies. Such a dual beam instrument with ratio recording, yields directly the difference in absorbance between two solutions as a function of wavelength. Because the absorption of proteins and some ligands is intense below 250 mμ, and because the absorptivities of the bands to be studied are not especially great, problems of resolution and sensitivity arise which restrict the applicability of the method. In the following sections a brief discussion of the factors involved is given (*A*, *B*, *C*), experimental variables are optimized (*D*), and criteria for successful use of the method are derived (*E*).

A. Relations among Shortest Accessible Wavelength, Resolution, and Solution Absorbance

Equation 1 expresses the total light flux $I_o(\lambda)$ incident upon the absorption cells in terms of the optical parameters of the source and the monochromator:

$$I_o(\lambda) = B(\lambda) \cdot f \cdot g(\lambda) \cdot W^2 \cdot d\lambda/dx \tag{1}$$

where $B(\lambda) \equiv$ spectral brightness of the source lamp in flux per unit area of source per unit solid angle per infinitesimal wavelength interval, $f \equiv$ product of the slit height and the solid angle which the monochromator accepts, $g(\lambda) \equiv$ fraction of spectral flux at entrance slit which is transmitted to exit slit, $W \equiv$ width of (entrance and exit) slits, $d\lambda/dx \equiv$ reciprocal of the dispersion.

In the Cary Model 14 the slit-width is servo-controlled so as to vary the light flux through the reference cell with wavelength in such a way that the corresponding current through the photomultiplier is held constant. Since the light transmitted by the sample does not exceed that transmitted by the reference, this control criterion establishes a constant signal-to-noise ratio which is independent of wavelength. The photomultiplier current is given by

$$i = I_o(\lambda) \cdot 10^{-A_R(\lambda)} \cdot m(\lambda) \cdot G \tag{2}$$

where $A_R(\lambda) \equiv$ absorbance in the path of the reference beam, $m(\lambda) \equiv$ spectral sensitivity of the light-emissive surface of the photomultiplier, $G \equiv$ gain of the

[1] Back donation, which occurs to less extent in Fe (III) than Fe (II), would also have a spectral influence.

photomultiplier. Under conditions where current and all instrumental parameters except slit width are fixed, equations 1 and 2 show that

$$W^2 = C(\lambda) \cdot 10^{A_R(\lambda)} \tag{3}$$

where $C(\lambda) \equiv i[B(\lambda) \cdot f \cdot g(\lambda) \cdot d\lambda/dx \cdot m(\lambda) \cdot G].^{-1}$

As a consequence of equation 3, two problems arise in the spectrophotometry of intensely absorbing solutions: (*a*) As A_R increases with decreasing λ, a wavelength λ_m will be reached where W is the maximum width (3 mm for Cary 14) to which the slits open. Thus, normal operation of the spectrophotometer restricts the accessible spectral region at the short wavelength end. Since protein and ligand absorbances are the major contributors to the total absorbance at these wavelengths, a compromise must be made between the magnitude of the difference absorbance signal and the minimum wavelength of the spectral scan. (*b*) As W increases with decreasing λ, the spectral bandwidth (polychromaticity) increases. Unless the spectral bandwidth remains less than the width of the absorption band, an accurate record of the absorbance will not be obtained.

It would be useful to investigate means of increasing the source brightness $B(\lambda)$ and the photomultiplier spectral sensitivity $m(\lambda)$ for wavelengths less than 250 mμ. Such improvements could be made without altering the optical system of the Cary 14, but not without limit because stray light will ultimately introduce significant errors (Sandberg, 1967). A deuterium lamp UV source, which is somewhat more intense than the standard hydrogen lamp, was used for all experiments reported here.

B. Relations among Extent of Complex Formation, Ligand Concentration, and Cell Path Length

With the assumption that a single dissociation constant, K_d, describes the equilibrium among ligand, hemeprotein, and complex, and for the condition that the concentration C_L of ligand is much larger than the total (free plus occupied) concentration of binding sites C_H, the extent of complex formation is given by

$$C_X/C_H = (1 + K_d/C_L)^{-1} \tag{4}$$

where C_X is the concentration of complexed sites. Note that the fraction of formation depends only upon ligand concentration. The extent of formation can be increased without changing the absorbance contributions of the ligand and protein by concentrating the latter two components d times and decreasing the cell path length by the same factor d.

C. Errors in the Difference Absorbance

When a ligand which absorbs significantly is to be the complexing agent, a tandem configuration is required as in Fig. 1 where cell 4 is used to balance out the ligand

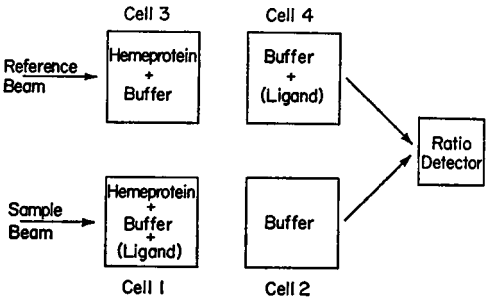

FIGURE 1 Description of tandem cell arrangement for difference spectroscopy. The numbering convention for the cells is shown. The components of the solutions in each cell are indicated. The brackets indicate that the ligand is added after a baseline is recorded.

contribution at cell 1. In the following treatment of errors arising from path length and pipetting differences, the absorbances of only the protein and ligand are considered and these are taken to obey Beer's law. Prior to the addition of ligand, a baseline is recorded which corresponds to the difference absorbance

$$A_o = \epsilon_H C_H^0 \Delta b_{13} \tag{5}$$

where $\epsilon_H \equiv$ absorptivity per (uncomplexed) binding site, $C_H^0 \equiv$ initial binding site concentration (same solution is used in cells 1 and 3), $\Delta b_{13} \equiv$ path length difference $(b_1 - b_3)$. (Numerical subscripts will refer to cells defined in Fig. 1.) After addition of ligand to cells 1 and 4, and buffer to cell 3, the difference absorbance is

$$A_X = \epsilon_X C_{X1} b_1 + \epsilon_H (C_{H1} - C_{X1}) b_1 + \epsilon_L (C_{L1} - C_{X1}) b_1 - \epsilon_H C_{H3} b_3 - \epsilon_L C_{L4} b_4 \tag{6}$$

where $\epsilon_X \equiv$ absorptivity of the complex per site, $b \equiv$ path length, $\epsilon_L \equiv$ absorptivity of ligand, and C_H, C_L are total (bound plus free) concentrations.

It is convenient to define the dilution factors

$$\beta_i \equiv V_{Hi}/(V_{Hi} + V_{Li}) \tag{7}$$

where V_{Hi} and V_{Li} are the volumes of protein and ligand or buffer, respectively, which have been added to cell i, and then to define the differences in dilution factors

$$\Delta\beta_{ij} \equiv \beta_i - \beta_j \tag{8}$$

for ligand between cells 1 and 4 and for protein between cells 1 and 3. When relations 7 and 8 are used in 6, and only first-order differences are retained, the difference absorbance is given by

$$A_X = (\epsilon_X - \epsilon_H)\beta_1 C_H^0 b_1 + \epsilon_H \beta_1 C_H^0 \Delta b_{13} + \epsilon_H C_H^0 b_1 \Delta\beta_{13} + \epsilon_L (1 - \beta_4) C_{L*} \Delta b_{14} - \epsilon_L C_{L*} b_1 \Delta\beta_{14} \tag{9}$$

where C_{L_s} is the concentration of the ligand "stock" solution and two simplifying assumptions have been made: (*a*) $C_{X1} = \beta_1 C_H^0$ (full formation of complex), and (*b*) $C_L \gg C_H^0$. Relative to the baseline, the difference absorbance is

$$\begin{aligned}\Delta A &\equiv A_X - A_o \\ &= (\epsilon_X - \epsilon_H)\beta_1 C_B^0 b_1 + \epsilon_H(\beta_1 - 1)C_H^0 \Delta b_{13} + \epsilon_H C_H^0 b_1 \Delta\beta_{13} \\ &\quad + \epsilon_L(1 - \beta_4)C_{L_s}\Delta b_{14} - \epsilon_L C_{L_s} b_1 \Delta\beta_{14}. \end{aligned} \tag{10}$$

The first term is the desired difference spectrum and the other four terms are errors arising from path length and dilution differences. At the short wavelength limit ($\sim$210 mμ), the absorptivities of protein ($\epsilon_H \sim 1 \times 10^6$ M^{-1} cm^{-1}) and ligands ($\epsilon_L \sim 10$ to 10^4 M^{-1} cm^{-1}), and hence the errors, are greatest. In typical experiments $\beta \sim 0.99$, $b \leqq 1$ cm, $\epsilon_X - \epsilon_H \sim 10^{-2}\epsilon_H$, $\Delta b \leqq \frac{1}{5} \times 10^{-3}$ cm, and $\Delta\beta \leqq 3 \times 10^{-4}$. The ratio of the first three terms is then 10^4:15:300 and the signal is seen to predominate. This may or may not be the case for the last two terms, depending upon the ligand. In the case of azide, for example, $\epsilon_L = 2 \times 10^{-3}$ M^{-1} cm^{-1} and $C_{L_s} \sim 0.1$ M. For $C_H^0 = 2 \times 10^{-6}$ M, the ratio of the first term to the Δb_{14} and $\Delta\beta_{14}$ errors is 2×10^{-3}:3×10^{-3}:6×10^{-2}, and the final term (ligand pipetting error) can produce a difference absorbance in excess of the structurally induced change which one desires to record.

D. Optimization of Experimental Variables

The first term of equation 10, which will be denoted ΔA_S for signal, can be rewritten to include the extent of complex formation indicated by equation 5:

$$\Delta A_S = \Delta\epsilon C_H b/(1 + K_d/C_L) \tag{11}$$

where $\Delta\epsilon = \epsilon_X - \epsilon_H$ and $C_L \gg C_H$ (as before).

The absorbances of the protein in cell 3 and the ligand in cell 4 are given by $A_H = \epsilon_H C_H b$ and $A_L = \epsilon_L C_L b$, respectively, whence

$$\Delta A_S = \frac{\Delta\epsilon A_H A_L}{\epsilon_H(A_L + K_d\epsilon_L b)}. \tag{12}$$

As indicated by equation 3, the sum of the protein and ligand absorbances in the reference beam

$$A_T \equiv A_H + A_L \tag{13}$$

determines the minimum accessible wavelengths, λ_m, and hence is a fundamental parameter. We therefore define the ligand absorbance fraction

$$x \equiv A_L/A_T \tag{14}$$

and rewrite equation 12 in the form

$$\Delta A_B = \frac{\Delta\epsilon \cdot x(1 - x)A_T}{\epsilon_H\left(x + \frac{K_d\epsilon_L b}{A_T}\right)}. \tag{15}$$

The uncertainty in the difference absorbance, ΔA_B, is given, approximately, by the sum of two major contributions:

$$\Delta A_B = \beta E A_L + A_N \tag{16}$$

where E is the relative pipetting error, $\Delta\beta = -\beta(1 - \beta)E$, and A_N is the error due to the instrument noise. The signal-to-noise ratio (SNR) is defined as

$$\text{SNR} \equiv \Delta A_S/\Delta A_B \tag{17}$$

whence

$$\text{SNR} = \frac{\Delta\epsilon \cdot x(1 - x)}{\epsilon_H \cdot \beta \cdot E\left(x + \frac{K_d\epsilon_L b}{A_T}\right)\left(x + \frac{A_N}{\beta E A_T}\right)}. \tag{18}$$

It should be noted that $\Delta\epsilon$, x, ϵ_H, ϵ_L, and A_T are wavelength dependent. For the systems studied here, because conditions are worst at λ_m where ϵ_H and ϵ_L are largest and the permissible A_T is smallest, the spectrum will be detectable throughout the entire region if SNR exceeds 1 at λ_m. Reduction of path length, b, increases SNR as long as $K_d\epsilon_L b > A_L$, but for reasons of technique and solubility it is not practical to take $b < 0.05$ cm.

The optimum value of x is obtained from analysis of equation 18. First note that $x(1 - x)$ cannot exceed 0.25. Typical values of $\Delta\epsilon/\epsilon_H$ (at λ_m), β, and E in these experiments are 6×10^{-3}, 0.99, and 0.03, respectively. From this

$$\frac{\Delta\epsilon \cdot x(1 - x)}{\epsilon_H \beta E} \leqq 0.05 \tag{19}$$

and for SNR $\geqq$ 1, equation 18 requires $x < 0.2$. Maximization of SNR yields an optimum value, x_{opt}, which for these small values (<0.2) is given approximately by

$$x_{\text{opt}} \approx \left[\frac{(K_d\,\epsilon_L\, b/A_T)(A_N/\beta E A_T)}{1 + (K_d\,\epsilon_L\, b/A_T)(A_N/\beta E A_T)}\right]^{1/2}. \tag{20}$$

Equation 20 expresses the best distribution of absorbance between protein and ligand.

E. Criteria for Successful Application to a Particular Complex

Although SNR must certainly be greater than one, we would much prefer SNR to exceed 10 throughout the spectral region. In such a case, equation 18 in reciprocal form becomes

$$\frac{\epsilon_H \beta E}{\Delta\epsilon \cdot x(1-x)}\left\{x^2 + x\frac{A_N}{\beta E A_T} + x\frac{K_d\,\epsilon_L\,b}{A_T} + \left(\frac{K_d\,\epsilon_L\,b}{A_T}\right)\left(\frac{A_N}{\beta E A_T}\right)\right\} < 0.1. \quad (21)$$

For this inequality to hold, each of the four terms on the left must separately be less than 0.1. From the first term $x^2 < 0.005$ or $x < 0.07$. The following relations come from the second and third terms.

$$\frac{\epsilon_H A_N}{\Delta\epsilon(1-x)A_T} < 0.1 \quad (22)$$

$$\frac{\epsilon_H \beta E K_d\,\epsilon_L\,b}{\Delta\epsilon(1-x)A_T} < 0.1 \quad (23)$$

A_m, the value of $A_T(\lambda_m)$ which results in maximum slit width, is about 2 absorbance units at 210 mμ. A_N is usually under 0.003, but not better than 0.001. From this, the following expression is obtained:

$$0.1 < \left(\frac{\epsilon_H A_N}{\Delta\epsilon(1-x)A_T}\right)_{\lambda_m} < 0.3. \quad (24)$$

In these experiments, therefore, the inequality (22) does not hold at the shortest wavelengths, and one cannot expect to achieve a SNR of 10:1 in that spectral region.

When the inequality (23) is evaluated at λ_m, the following relation is found:

$$K_d\epsilon_L(\lambda_m) < A_m/50b = 0.02A_m/b. \quad (25)$$

Hence, weakly bound and strongly absorbing ligands may be excluded.

If a ligand is of limited solubility, it may not be possible to obtain a useful SNR even though the ligand meets criterion 25. This can be seen when $A_L(\lambda_m)/x(\lambda_m)$ from relation 14 is substituted for A_m in inequality 25:

$$50\frac{x(\lambda_m)}{1-\beta}K_d < C_{Ls}. \quad (26)$$

Because the absorbance $A_H{}^0$ must be recorded down to λ_m prior to addition of ligand, the protein concentration is limited by $A_H{}^0(\lambda_m) \leqq A_m$. After the dilution attendant ligand addition,

$$A_H(\lambda_m) = \beta A_H{}^0(\lambda_m) = \{1 - x(\lambda_m)\}A_m \leqq \beta A_m. \quad (27)$$

Thus, $1 - \beta \leqq x(\lambda_m)$ and from equation 26

$$50K_d < C_{L_0}, \tag{28}$$

a criterion which sets a lower limit on the saturation concentration of ligand.

MATERIALS AND METHODS

A. Hemeproteins

Bacterial micrococcus catalase (BMC) was prepared in this laboratory from *Micrococcus lysodeikticus* (American Type Culture Collection No. 4698, American Type Culture Collection, Rockville, Md.) grown in submerged culture (Beers, 1955). The enzyme was extracted by the method of Herbert and Pinsent (1948) and purified by ammonium sulfate fractionation, acetone precipitation from neutral 0.01 M phosphate buffer, and gel filtration. All preparations used here had purity values (defined for BMC as the ratio $A_{406\ m\mu}/A_{280\ m\mu}$) greater than 0.90. At pH 7 we determined the Soret absorptivity (λ_{max} = 406 mμ) to be 102.(7) mM^{-1} cm^{-1} (heme concentration) from parallel measurements of absorbance, iron concentration (as *o*-phenanthroline complex), and heme concentration (as pyridine hemochromogen), and thereafter computed the enzyme concentration from the Soret absorbance.

Horseradish peroxidase (HRP) was obtained from Worthington Biochemical Corporation, Freehold, N. J. The purity value ($A_{403\ m\mu}/A_{275\ m\mu}$ for HRP) was greater than 2.9 for lot HPO – FF 6550. At pH 5.6, the Soret absorptivity (λ_{max} = 403 mμ) is 91 mM^{-1} cm^{-1} (Keilin and Hartree, 1951) and was used to determine concentration.

Horse heart ferrimyoglobin (MetMb) was obtained from Nutritional Biochemicals Corporation, Cleveland, Ohio (lot 5589) and used without further purification. A slight molar excess of potassium ferricyanide was added to each stock solution to insure complete formation of the ferric form, and then the stock solution was dialyzed against the desired buffer. The ratio $A_{409\ m\mu}/A_{280\ m\mu}$ was 5.0 at pH 6.8. At pH 6.4, the Soret absorptivity is 188 mM^{-1} cm^{-1} (Scheler, Schoffa, and Jung, 1957) and was used to determine concentration.

Horse ferrihemoglobin (MetHb) was obtained from Mann Research Laboratories, Inc., New York (lot N 1716) and used without further purification. (Commercially available hemoglobin is known to be chromatographically heterogeneous [Sober and Peterson, 1960]. The differences reflected by this separation method would not be expected to influence the experiments reported here.) Stock solutions were treated with ferricyanide as in the case of MetMb. The ratio $A_{405\ m\mu}/A_{275\ m\mu}$ was greater than 4.1. At pH 6.4, the Soret absorptivity is 179 mM^{-1} cm^{-1} (heme) (Scheler, Schoffa, and Jung, 1957) and was used to determine concentration.

B. Hemin

Hemin chloride was obtained from Mann Research Laboratories (lot H 1369) as recrystallized, cp, iron analysis 9.2% (theoretical 8.6%), and used without further purification.

C. Ligands

Sodium azide, "purified" grade, was obtained from Fisher Scientific Company, New York (lot 722481). Potassium cyanide, certified reagent grade, was also obtained from Fisher (lot 730137).

D. Absorption Cells

These were produced by Pyrocell Manufacturing Company, Westwood, N. J., with windows of far-UV (S18-260) silica, in sets of four matched to within 2% transmission at 220 mμ. The optical path length between inside faces of the windows is ±0.005 mm of nominal length. A set of precision (±0.0025 mm) two-way silica (S18-260) inserts was used to reduce the optical path length to either 0.05 or 0.20 cm (±0.0075 mm).

E. Precautions with Cyanide and Azide

Fresh stock solutions of these ligands were prepared prior to the experiments because of decomposition. Since hydrocyanic and hydrazoic acids dissociate only weakly (with pK's of 9.3 and 4.7, respectively) a buffering capacity equal to or somewhat greater than the total equivalents of ligand added was necessary to prevent pH changes and possible concomitant spectral changes. The addition of KCN to a solution at pH 6.7, for example will result in the escape of HCN gas. We assume that the attendant error in cyanide concentration is negligible but did cover the cells to avoid transfer of HCN gas.

F. Temperature Control

To prevent spectral differences which might arise from temperature differences between the hemeprotein solutions, the stock solutions were equilibrated at room temperature and cell compartments were maintained at 25 ± 1°C.

G. Scanning Rate

Because the slit-width changes markedly when a far UV difference spectrum is run, the rate of scan of the monochromator must be slow enough for the slit-servo to follow. In these studies, therefore, the scan rate, 5 A/sec was slower than the normal rate–which is usually chosen equal to or greater than the ratio of the spectral bandwidth to the pen period. The spectral bandwidth was 40–50 A at the shortest wavelengths, decreasing rapidly with increasing wavelength.

H. Example of Measurement

For a path length of 0.005 cm, 1.00 ml of hemeprotein solution is delivered with a volumetric pipette to cells 1 and 3 (Fig. 1). Cells 2 and 4 receive 1.00 ml of buffer. After the baseline is recorded, 10 λ of ligand solution is added to cells 1 and 4 and 10 λ of buffer is added to cell 3, the contents are stirred, and the difference spectrum run.

RESULTS

A. Spectra of BMC Complexes

In Figs. 2, 3, and 4, the spectra of several complexes of BMC are shown in the UV, visible, and IR regions. The cyanide UV data is in agreement with previously published spectra (Chance and Herbert, 1950; Brill and Williams, 1961). Magnetic suceptibility measurements on complexes of BMC have not yet been reported, but data of this kind is available for other catalases.

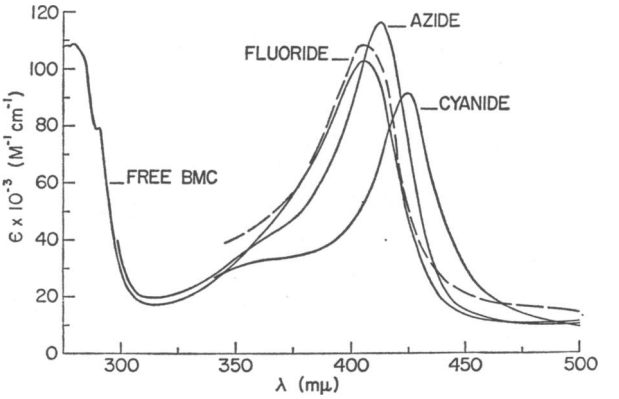

FIGURE 2 Ultraviolet spectra of free BMC and fluoride, azide, and cyanide complexes (275–500 mμ). For the azide complex, the pH was 7.1 and the azide/heme ratio was 3800. For the cyanide complex, the pH was 7.7 and the cyanide/heme ratio was 920. For the fluoride complex, the pH was 4.5 and the fluoride/heme ratio was 7000. For free BMC, the pH was 7.0. In all of these measurements, the heme concentration was between 6.5 and 7.1 μM.

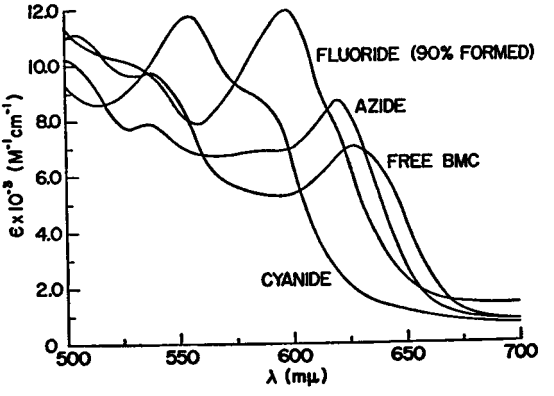

FIGURE 3 Visible spectra of free BMC and fluoride, azide, and cyanide complexes (500–700 mμ). The concentration of the fluoride complex was about 90% of the total heme concentration. For the azide complex, the pH was 7.1 and the azide/heme ratio was 440. For the cyanide complex, the pH was 7.6 and the cyanide/heme ratio was 82. For the fluoride complex, the pH was 4.9 and the fluoride/heme ratio was 710. For free BMC, the pH was 7.0. In all of these measurements, the heme concentration was between 67 and 71 μM.

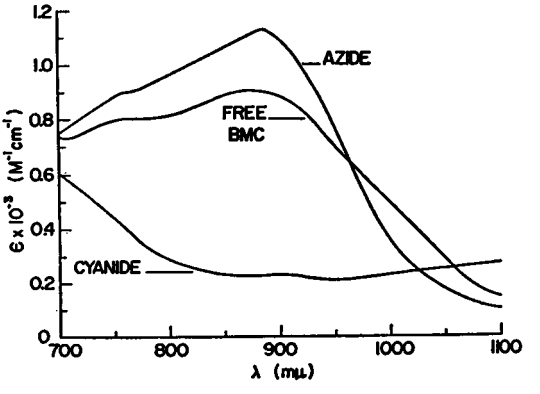

FIGURE 4 Near infrared spectra of free BMC and azide and cyanide complexes (700–1100 mμ). For the azide complex, the azide/heme ratio was 28. For the cyanide complex, the cyanide/heme ratio was 17. In all of these measurements, the heme concentration was between 340 and 360 μM and the pH was 7.0.

B. Dissociation Constants of Hemeprotein Complexes

The selection of ligands which are suitable for difference spectroscopy below 250 mμ is based upon the criteria derived above:

$$50\ K_d \cdot \epsilon_L(\lambda_m) \cdot b/A_m < 1 \tag{25'}$$

$$\text{saturation concentration of ligand} > 50\ K_d \tag{28'}$$

An additional criterion is that the magnetic moments of most of the corresponding hemeprotein complexes be known. Five ligands for which the latter is true are fluoride, cyanate, thiocyanate, azide, and cyanide. Table I lists the absorptivities at 210 mμ of these ligands; the largest among the reported dissociation constants

TABLE I

AN EVALUATION OF CRITERIA 25′ AND 28′ FOR SELECTION OF LIGANDS BASED UPON DATA FROM THE LITERATURE

Ligand	* $\epsilon_{210\ m\mu}$	‡ K_d	§ $50\ K_d \cdot \epsilon_L(\lambda_m) \cdot b/A_m$	$50\ K_d$
	$M^{-1}cm^{-1}$	M		M
Fluoride	0.2	1.6×10^{-2} (MetMb)	4.0×10^{-3}	0.80
Cyanate	31	4.2×10^{-3} (MetMb)	0.17	0.21
Thiocyanate	2.9×10^4	4.5×10^{-3} (MetMb)	165	0.23
Azide	2×10^3	6.8×10^{-6} (MetMb)	0.17	3.4×10^{-3}
Cyanide	7.1	1.8×10^{-5} (MetMb)	1.6×10^{-4}	9×10^{-4}

* Buck, Singhadeja, and Rogers (1954); Sandberg (1967).
‡ 22°C, pH 7.0; Blanck, Graf, and Scheler (1961).
§ For $b = 0.05$ cm and $A_m = 2.00$.

of the complexes with horse liver catalase (HLC), MetMb, and MetHb (which happens to be the MetMb complex in each case); the corresponding values of $50\ K_d \cdot \epsilon_L(\lambda_m) \cdot b/A_m$ (for the conditions $b = 0.05$ cm and $A_m = 2.00$) and $50\ K_d$. Clearly thiocyanate violates criterion 25′. Fluoride does not satisfy criterion 28′ because of its limited solubility and cyanate is marginal with respect to both criteria. Azide satisfies the first criterion marginally and the second well. Cyanide is certainly the most suitable ligand.

Having put aside fluoride, cyanate, and thiocyanate on the basis of data from the literature, we then measured the apparent dissociation constants of the azide and cyanide complexes of BMC, HRP, MetMb, and MetHb under the experimental conditions to be used for recording the difference spectra so that the criteria 25′ and 28′ could be evaluated with precision. The concentration of complex, C_X, was calculated for each ligand concentration, C_L, from the measured absorbances at the wavelengths in the Soret region. K_d was then computed by an iterative method which derives its corrections from a least square fit of equation 4

TABLE II

APPARENT DISSOCIATION CONSTANTS AND EVALUATION OF CRITERIA 25′ AND 28′ FOR CYANIDE AND AZIDE COMPLEXES OF BMC, HRP, MetHb, AND MetMb

	Cyanide complex			Azide complex		
		$*50\ K_d \cdot \epsilon_L(\lambda m) \cdot b$			$*50\ K_d \cdot \epsilon_L(\lambda m) \cdot b$	
Hemeprotein	K_d	A_m	$50\ K_d$	K_d	A_m	$50\ K_d$
	M, 25°C		M	M, 25°C		M
BMC, pH 6.7	1.4×10^{-5}	1.2×10^{-4}	7.0×10^{-4}	6.8×10^{-4}	1.7	3.4×10^{-2}
HRP,						
pH 6.7	4.4×10^{-6}	3.9×10^{-5}	2.2×10^{-4}	$\sim 1 \times 10^{-1}$	$\sim 2.5 \times 10^{2}$	~ 5
pH 4.7	—	—	—	$\sim 2 \times 10^{-2}$	~ 50	~ 1
MetHb,						
pH 6.7	5.6×10^{-6}	5.0×10^{-5}	2.8×10^{-4}	1.6×10^{-5}	4.0×10^{-2}	8.0×10^{-4}
MetMb,						
pH 6.7	1.5×10^{-5}	1.3×10^{-4}	7.5×10^{-3}	5.9×10^{-5}	0.15	3.0×10^{-3}

* For $b = 0.05$ cm, $A_m = 2.00$.

to the values of C_X/C_H determined at each C_L (Sandberg, 1967). (The heme groups are assumed to be independent in BMC and MetHb.) In the case of cyanide, the ligand concentration is reduced at an unknown rate due to evolution of HCN gas. This error would tend to increase the value of the apparent dissociation constant. The values of K_d are listed in Table II. In general, our values of MetMb and MetHb complexes agree with those in the literature (Blanck, Graf, and Scheler, 1961; Havemann and Haberditzl, 1958; Havemann and Hirse, 1955). Because it was not possible to produce full formation of the azide complex of HRP, the value for K_d given in Table II is approximate.

Evaluation of criteria 25′ (for $b = 0.05$ cm and $A_m = 2.00$) and 28′ is given in Table II. The cyanide complexes of all four hemeproteins meet both requirements as do the azide complexes of MetMb and MetHb. HRP-azide, at pH 6.7 and 4.7 does not satisfy either criterion. BMC-azide marginally satisfies the first requirement, and it would be helpful to find conditions where K_d is smaller. In the case of horse blood catalase (HBC), the apparent dissociation constant decreases with decreasing pH (Chance, 1952), but BMC is not sufficiently soluble in pH 4.7 acetate buffer (the isoelectric point is 4.5; Sandberg, 1967) for this effect to be useful.

C. Shape of Difference Spectra

An absorption band can be characterized by the wavelength and absorptivity of of the maximum, and by the bandwidth. Donovan, Laskowski, and Scheraga (1961) have made a theoretical analysis of the difference spectrum which arises when a single

absorption band of constant absorptivity and width undergoes a wavelength shift. For small shifts, the difference spectrum is approximately proportional to the first derivative of the absorbance, while for shifts which are much greater than the bandwidth, the positive difference absorbance will have the appearance of a normal absorption band. When the bandwidth changes along with a small wavelength shift, the difference spectrum exhibits two nodes. When wavelength, absorptivity, and width all change, or when more than one band is involved, the shape of the difference spectrum can be complicated.

The appearance of a new band or the disappearance of a band in the absolute spectrum is, of course, reflected in the difference spectrum.

D. Biscyanoferriprotoporphyrin

The difference spectrum for biscyanoferriprotoporphyrin vs. hematin shows positive absorption in the region 210–249 mμ with $\Delta\epsilon_{213\ m\mu} = 6.4\ mM^{-1}\ cm^{-1}$; and a trough with $\Delta\epsilon_{265\ m\mu} = -2.0\ mM^{-1}\ cm^{-1}$ (Brill and Sandberg, 1967).

E. MetMb-CN and MetHb-CN

The cyanide complexes of all the hemeproteins show difference absorption bands in the region 210–250 mμ. Typical spectra for MetMb-CN and MetHb-CN, for which the coordination of the iron is known, are shown in Fig. 5. Each spectrum has three bands, and these are seen to correspond closely in wavelength and absorptivity from protein to protein. The pairs of bands at 213 and 235 mμ differ only in absorptivity while bands of intermediate energy differ in location, 223 mμ for MetHb-CN and ~227 mμ for MetMb-CN. The longest wavelength bands have $\Delta\epsilon_{235\ m\mu} = 9.7^{+1.5}_{-1.3}\ mM^{-1}\ cm^{-1}$ for MetHb-CN (where +1.5 and −1.3 specify the range of the measured difference absorptivity values) and $\Delta\epsilon_{235\ m\mu} = 11.7^{+0.3}_{-0.4}\ mM^{-1}\ cm^{-1}$ for MetMb-CN. MetHb-CN has a trough at 262 mμ, while the MetMb-CN difference absorbance flattens out in this region.

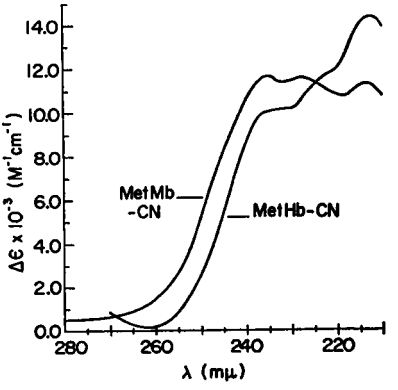

FIGURE 5 Ultraviolet difference spectra of MetHb-CN and MetMb-CN (280–210 mμ). For MetHb-CN, the heme concentration was 54 μM; cyanide 30 mM; path length 0.05 cm; and pH 6.7. For MetMb-CN, the heme concentration was 99 μM; cyanide 30 mM; path length 0.05 cm; and pH 6.7.

F. HRP-CN and BMC-CN

Unfortunately, the difference spectra of BMC-CN and HRP-CN could not be obtained below 220 mμ due to the larger molecular weight per heme group. For the region 220–280 mμ, typical spectra are shown in Fig. 6. HRP-CN has difference bands at 235 and ~226 mμ which are similar to those of MetHb-CN and MetMb-CN, and the difference absorbance is increasing at 220 mμ so that the possibility of a maximum in the 215 mμ region is not excluded. For HRP-CN, $\Delta\epsilon_{235\ m\mu} = 5.8^{+0.6}_{-0.5}$ $mM^{-1}\ cm^{-1}$. Because of a rapid increase of absorptivity, the details of the difference spectrum of BMC-CN below 230 mμ are obscure. However, the companion to the 235 mμ bands in the cyanide complexes of the other three proteins is clearly

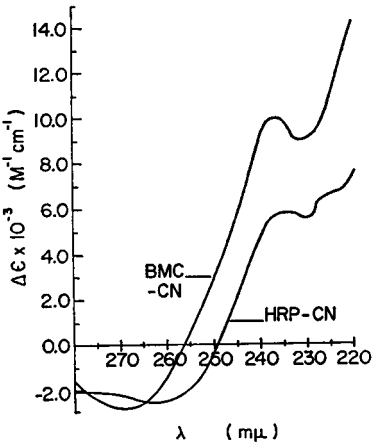

FIGURE 6 Ultraviolet difference spectra of MetHb-N_3 and MetMb-N_3 (280–210 mμ). For MetHb-N_3, the heme concentration was 60 μM; azide 3 mM; path length 0.05 cm; and pH 6.7. For MetMb-N_3, the heme concentration was 99 μM; azide 30 mM; path length 0.05 cm; and pH 6.7.

present, peaking at 236 mμ with $\Delta\epsilon_{236\ m\mu} = 12.0^{+1.9}_{-1.8}$ $mM^{-1}\ cm^{-1}$. Both HRP-CN and BMC-CN show troughs at 260–270 mμ very like that of biscyanoferriprotoporphyrin vs. hematin.

G. MetMb-N_3 and MetHb-N_3

It was difficult to record the difference spectra of MetMb-N_3 and MetHb-N_3 for an unexpected reason. The difference absorbance in the region 210–250 mμ was time dependent. It has since been learned that azide reacts with methionine residues, and indeed will inactivate HRP by this mechanism (Brill and Weinryb, 1967). The difference spectra were, therefore, recorded immediately upon formation of the complex. Typical spectra are shown in Fig. 7. MetMb-N_3 have similar bands, located at 241 and 242 mμ, respectively, with $\Delta\epsilon_{241\ m\mu} = 11.8$ $mM^{-1}\ cm^{-1}$ and $\Delta\epsilon_{242\ m\mu} = 8.2^{+0.9}_{-0.6}$ $mM^{-1}\ cm^{-1}$. In addition a difference band at about 280 mμ is indicated, and below 220 mμ the difference absorbance increases rapidly.

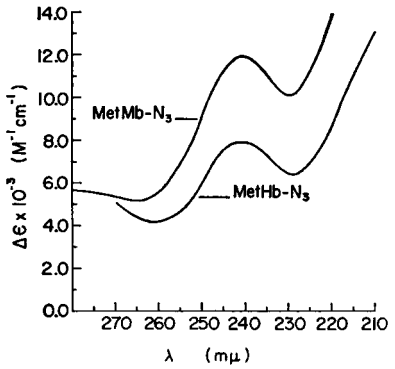

FIGURE 7 Ultraviolet difference spectra of BMC-CN and HRP-CN (280–220 mμ). For BMC-CN, the heme concentration was 3.6 μM; cyanide 3.3 mM; path length 1.0 cm; and pH 6.5. For HRP-CN, the heme concentration was 6.0 μM; cyanide 30 mM; path length 1.0 cm; and pH 6.7.

H. BMC-N_3

The difference spectrum of BMC-N_3 was also time dependent. However, no difference bands were observed in the spectrum recorded immediately after the complex was formed even though the concentration of azide exceeded the amount necessary for 95% formation. The positive difference absorbance in the region 260–270 mμ found in the MetMb-N_3 and MetHb-N_3 complexes was not present here.

DISCUSSION

A. Relation of Porphyrin Absorption Bands to the Spin State of the Iron-Ion Soret Band

The spectral behavior of absorption bands arising from transitions involving orbitals of ligands 5 and 6 or hybrid orbitals of ligand and metal should have analogies in the behavior of the corresponding types of porphyrin bands. It is generally agreed that the Soret band is a π-π^* transition involving porphyrin orbitals (among recent discussions are Brill and Williams, 1961; Offenhartz, 1965; Weiss, Kobayashi, and Gouterman, 1965). A review of the electronic structure, the predicted paramagnetic susceptibilities, and the absorption spectra of hemeprotein complexes has been given by George, Beetlestone, and Griffith (1961). An extensive study of a large number of complexes of MetHb and MetMb has shown that the locus of points which relate the wavelengths of the Soret band maxima with the magnetic susceptibilities of the complexes is a straight line, where low spin is associated with long wavelength (Scheler, Schoffa, and Jung, 1957). This behavior is also exhibited by the complexes of HRP and BMC (Table III). Note that the magnetic susceptibilities of HBC complexes are given since this data is not yet available for BMC. The basic molecular properties of the two catalases are similar. While susceptibility measurements have not been reported for biscyanoferriprotoporphyrin, one would expect it to be a low-spin complex, and this is indicated by the location of the Soret band maximum at the long wavelength of 420 mμ.

TABLE III

LOCATION OF ABSORPTION MAXIMA AND SHOULDERS* IN THE VISIBLE AND NEAR ULTRAVIOLET SPECTRA, AND MAGNETIC MOMENTS OF HEMEPROTEIN COMPLEXES‡

Hemeprotein	λ_{max} of Absorption bands					Magnetic moment
	C.T. 1	α	β	C.T. 2	Soret	
	mμ	*mμ*	*mμ*	*mμ*	*mμ*	*Bohr magnetons*
			Free hemeprotein			
BMC, pH 7.0	627.5	—	537	504	406	5.7 (HBC§)
HRP, pH 5.6	641	(~580)	(~530)	497	403	5.4
MetMb, pH 6.4	630	(580)	(550)	502	408	5.8
MetHb, pH 6.4	631	(575)	(540)	500	404.5	5.7
			Fluoride complex			
BMC	598	—	(~535)	485	406.5	5.7 (HBC)
HRP	612	560	(530)	488	404	5.9
MetMb	604	(585)	(550)	487	406	5.9
MetHb	605	—	(550)	482.5	403	5.9
			Azide complex			
BMC	621	587	537.5	500	413	5.5 (HBC)
HRP	635	(565)	534	(~495)	416	No data
MetMb	(635)	570	540	—	420	3.4
MetHb	(630)	575	540	—	417	2.8
			Cyanide complex			
BMC	—	(~588)	554.5	—	425	2.4 (HBC)
HRP	—	(570)	538	—	423	2.8
MetMb	—	(570)	540	—	422	2.3
MetHb	—	(~575)	540	—	419	2.6

* In parentheses.

‡ Averages of data from the following references: Hartree, 1946; Theorell and Ehrenberg, 1951, 1952; Deutsch and Ehrenberg, 1952; Scheler, Schoffa, and Jung, 1957; Havemann and Haberditzl, 1958; Beetlestone and George, 1964.

§ Horse blood catalase.

Infrared Bands. Additional evidence to support the assignment of the magnetic susceptibilities of BMC complexes comes from the near infrared spectra shown in Fig. 4. MetMb-F has a band at about 850 mμ with a shoulder at about 750 mμ while MetMb-CN does not have any bands in this region (Hanania, 1953). Similarly free BMC has a band at about 870 mμ with a shoulder at 750 mμ while BMC-CN has no bands in this region. Furthermore, BMC-N_3 also has a band at

880 mμ with a shoulder at about 760 mμ. Thus, extension of the magnetic data from HBC complexes to BMC complexes has support in the behavior of the near infrared spectra.

Visible Bands. The visible bands of the hemeprotein complexes also change with the magnetic susceptibility. In general, bands (C.T.1) between 600 and 650 mμ and bands (C.T.2) between 480 and 510 mμ are observed in high-spin complexes. Bands (α) between 555 and 600 mμ and bands (β) between 525 and 555 mμ are observed in low-spin complexes (Table III). Complexes of intermediate spin have most or all of these bands. Several explanations of the structural properties of complexes of intermediate susceptibilities have been advanced (Havemann and Haberditzl, 1958; George, Beetlestone, and Griffith, 1961; Beetlestone and George, 1964; Schoffa, 1964). George and coworkers have observed a temperature dependence in the visible bands of MetMb complexes of intermediate values of magnetic susceptibility, and have therefore suggested that these complexes are mixtures of high- and low-spin states in thermal equilibrium.

The likeness of the visible spectra of MetMb and MetHb complexes indicates that the heme environments should be very similar in these two proteins. This conclusion is supported by the molecular structures in the crystalline state as revealed by X-ray diffraction. Spectral differences in the visible between HRP complexes and those of the globins are few. BMC complexes show further differences.

B. Identification of Chromophores Responsible for UV Difference Spectral Changes

Hematin is of intermediate spin (Hartree, 1946) and it is not surprising to find a diffuseness of absorption. There is a broad and poorly defined set of bands absorbing between 210 and 245 mμ, and a less intense, but better defined band between 245 and 290 mμ with a maximum of $\Delta\epsilon_{254\ mu} = 19\ mM^{-1}\ cm^{-1}$. Conversion to the low-spin monomeric dicyanide complex strengthens the absorption in the former region and slightly attenuates it in the latter, the isosbestic point being 249 mμ. The difference peak at 213 mμ is flat, there being a shoulder at 222 mμ. Transitions in this wavelength region have been observed in ferric hexacyanide (Kiss, Abraham, and Hegedüs, 1940) and assigned as charge transfer from ligand to metal (Naiman, 1961). The data from hematin, biscyanoferriprotoporphyrin, and from the cyanide complexes of the hemeproteins presented above, are consistent with there being charge transfer transitions from cyanide and from porphyrin centered within the region 210–230 mμ. However, the protein-cyanide complexes exhibit a difference band at 235–238 mμ which is not present in biscyanoferriprotoporphyrin. We have proposed that this transition is associated with histidine coordinated to the iron (Brill and Sandberg, 1967).

The ligand in position 5 of the ferric ions in MetMb and MetHb is known to be an imidazole group from X-ray diffraction analysis. Histidine has one absorption

band above 185 mμ ($\epsilon_{211\ m\mu}$ = 5.9 M^{-1} cm^{-1}) (Sussman and Gratzer cited in Wetlaufer, 1962). A shift of this band or appearance of an essentially new (charge transfer) band toward longer wavelength is expected upon coordination to the metal ion. Data is not available on the behavior of the histidine band at 211 mμ upon formation of a high-spin complex. In the cyanide complexes of the heme proteins, any of the difference maxima at 213, 225, and 235 mμ could be associated with imidazole orbitals. However, the first two have alternative explanations and the last has not. The following factors lend support to the assignment of the 235 mμ absorbance to a transition which depends upon the presence of a histidine-heme bond: (*a*) All the difference spectra of low-spin complexes and compounds (Sandberg, 1967; Brill and Sandberg, 1967) vs. free hemeprotein (high-spin) exhibit maxima between 235 and 241 mμ (except BMC-II, 248 mμ); biscyanoferriprotoporphyrin vs. hematin does not. (*b*) Azide, which produces low-spin complexes with MetMb and MetHb, does not significantly lower the spin state of free BMC. Thus, appreciable electron delocalization, upon which the appearance of the "imidazole band" depends, is not present in BMC azide; and the band is predicted not to occur. It does not. (*c*) The band is of too great an intensity and too short a wavelength to arise from a metal *d-d* transition. The assignment to *d-d* or *d-p* absorption is also rendered very unlikely by the absence of the band in biscyanoferriprotoporphyrin.

Since both HRP-CN and BMC-CN have the band at 235 mμ, we suggest that histidine is in the coordination sphere of the iron in the enzymes as well as in Mb and Hb. The spectral and functional differences among the four hemeprotins would then be due to differences in near neighbors to the heme and/or tertiary structure.

The spectra of alkyl azides have weak ("forbidden") transitions at about 287 mμ (Closson and Gray, 1963). Counterparts of these bands are expected in low-spin azide complexes, and are likely to be more intense because of the distortion (Stryer, Kendrew, and Watson, 1964) from regular symmetry (Pauling and Brockway, 1937). The UV difference spectra of MetMb-N_3 and MetHb-N_3 indicate bands above 280 mμ, analogous to and stronger than those of the alkyl azides, and have the "imidazole band" at 240 mμ. The UV difference spectrum of the BMC-N_3 complex is in distinct contrast to the preceding spectra. The absence of all difference bands strongly supports the viewpoint presented here.

C. Relation between the Differences in Absorptivity and Magnetic Susceptibility

Proceeding from the hypothesis of George, Beetlestone, and Griffith (1961) that hemeprotein complexes are thermal mixtures of high-spin and low-spin states in equilibrium, we can attempt to relate the "imidazole" difference absorptivity to the excess population of molecules in the low-spin over those in the high-spin state.

The fraction Z of hemeprotein in the low-spin state is given by

$$Z = (\chi - \chi_h)/(\chi_l - \chi_h) \tag{29}$$

where χ is the observed susceptibility and χ_h and χ_l are the susceptibilities of pure high- and low-spin complexes, respectively. In difference spectroscopy, the absorbance of the complex (of susceptibility χ') is compared with the absorbance of free hemeprotein (of susceptibility χ''). Thus the important parameter is the difference ΔZ between the low-spin fractions of complexed and free protein.

$$\Delta Z = (\chi' - \chi'')/(\chi_l - \chi_h). \tag{30}$$

George et al. (1961) give $\chi_h = 14{,}800 \times 10^{-6}$ emu (the molar paramagnetic susceptibility of the ^6S state) and $\chi_l = 2120 \times 10^{-6}$ emu (spin doublet with some orbital contribution). The computed values of ΔZ are listed in Table IV together with the difference absorptivities of the "imidazole band." The intensity of this band is seen to be a monotonically increasing function of ΔZ. The only entry which deviates significantly is from MetMb-N_3, but this absorption is affected by overlap with the band at 280 mμ (Fig. 7). Since, in general, the absorption in the region 230–250 mμ contains contributions from changes in bands centered in the adjoining regions, it is not possible to determine accurately the difference absorptivity due to the "imidazole band" alone. Thus, while the ΔZ, $\Delta\epsilon$ couples of Table IV establish a relation between the magnetic and spectral changes, they cannot provide a critical check of the linearity which is required by the hypothesis of George et al.

TABLE IV

EXPERIMENTAL RELATION BETWEEN THE DIFFERENCE ABSORPTIVITY OF THE "IMIDAZOLE BAND" AND THE NET MOLE FRACTION OF A HEMEPROTEIN COMPLEX IN THE LOW-SPIN STATE

Complex	ΔZ	$\Delta\epsilon$
		$m\mu^{-1}cm^{-1}$
BMC-N_3	0.085	0
HRP-CN	0.72	5.8
MetMb-N_3	0.72	11.8
MetHb-N_3	0.83	8.2
MetHb-CN	0.87	9.7
BMC-CN	0.88	12.0
MetMb-CN	0.925	11.7

D. Related Experiments

The methods of this paper have been applied to the study of peroxide compounds of hemeproteins (Sandberg, 1967; Brill and Sandberg, 1967), and the results will be reported in detail at a later date.

Optical rotatory dispersion and circular dichroism, very important spectral properties complementary to the measurements treated here, are currently being investigated for hemeproteins and hemepeptides (see for example, Urry, 1967). In the interpretation of all advanced optical data, the central role of the absolute absorption spectra of the simplest model complexes should not be overlooked. For example, in ferriheme undecapeptide there is apparently no absorption band at 253 mμ while the circular dichroism curve shows an extremum. The transition responsible for this circular dichroism band is resolved in absolute absorption spectra both of the hematin solution described in this paper and of heme in organic solvents (Brill and Turley, unpublished data).

H. E. Sandberg was a Predoctoral Fellow of the U. S. Public Health Service during the period of this research, and the paper is drawn from his dissertation submitted to Yale University in partial fulfillment of the requirements for the Ph.D. degree.

This work was also supported by U. S. Public Health Service Research Grant GM-09256 from the Division of General Medical Science.

Reprint requests should be addressed to Prof. Brill in Virginia.

Received for publication 2 February 1968.

REFERENCES

BEERS, R. F., JR. 1955. *Science.* **122**:1016.
BEETLESTONE, J., and P. GEORGE. 1964. *Biochem.* **3**:707.
BLANCK, J., W. GRAF, and W. SCHELER. 1961. *Acta Biol. Med. Ger.* **7**:323.
BRILL, A. S., and H. E. SANDBERG. 1967. *Proc. Natl. Acad. Sci. U. S.* **57**:136.
BRILL, A. S., and I. WEINRYB. 1967. *Biochem.* **6**:3528.
BRILL, A. S., and R. J. P. WILLIAMS. 1961. *Biochem. J.* **78**:246.
BUCK, R. P., S. SINGHADEJA, and L. B. ROGERS. 1954. *Anal. Chem.* **26**:1242.
CHANCE, B. 1952. *J. Biol. Chem.* **194**:487.
CHANCE, B., and D. HERBERT. 1950. *Biochem. J.* **46**:402.
CLOSSON, W. D., and H. B. GRAY. 1963. *J. Am. Chem. Soc.* **85**:290.
DEUTSCH, H. F., and A. EHRENBERG. 1952. *Acta Chem. Scand.* **6**:1522.
DONOVAN, J. W., M. LASKOWSKI, JR., and H. A. SCHERAGA. 1961. *J. Am. Chem. Soc.* **83**:2686.
EDSALL, J. T. 1963. *In* Aspects of Protein Structure. G. N. Ramachandran, editor. Academic Press, Inc., New York. 179.
FISHER, H. F., and D. G. CROSS. 1965. *Arch. Biochem. Biophys.* **110**:217.
GEORGE, P., J. BEETLESTONE, and J. S. GRIFFITH. 1961. *In* Haematin Enzymes. J. E. Falk, R. Lemberg, and R. K. Morton, editors. Pergamon Press, Oxford, England. 105.
GIBSON, J. F., and D. J. E. INGRAM. 1957. *Nature.* **180**:29.
HANANIA, G. I. H. 1953. Ph.D. Thesis. The University of Cambridge, England. Reported in George et al., 1961.
HARTREE, E. F. 1946. *Ann. Rept. Progr. Chem. (Chem. Soc. London).* **43**:287.
HAVEMANN, R., and W. HABERDITZL. 1958. *Z. Physik. Chem. (Leipzig).* **209**:135.
HAVEMANN, R., and H. HIRSE. 1955. *Z. Physik. Chem. (Leipzig).* **204**:68.
HERBERT, D., and J. PINSENT. 1948. *Biochem. J.* **43**:193.
HERSKOVITS, T. T., and M. LASKOWSKI, JR. 1962. *J. Biol. Chem.* **237**:2481.
KEILIN, D., and E. F. HARTREE. 1951. *Biochem. J.* **49**:88.
KENDREW, J. C. 1962. *In* Enzyme Models and Enzyme Structure. Report of Symposium, Brookhaven National Laboratory, Upton, N. Y. 216.

KENDREW, J. C. 1963. *Science.* **139**:1262.
KISS, A. V., J. ABRAHAM, and L. HEGEDÜS. 1940. *Z. Anorg. Allgem. Chem.* **244**:98.
NAIMAN, C. S. 1961. *J. Chem. Phys.* **35**:323.
OFFENHARTZ, P. O'D. 1965. *J. Chem. Phys.* **42**:3566.
PAULING, L., and L. O. BROCKWAY. 1937. *J. Am. Chem. Soc.* **59**:13.
SANDBERG, H. E. 1967. Ph.D. Dissertation. Yale University, New Haven, Conn.
SCHELER, W., G. SCHOFFA, and F. JUNG. 1957. *Biochem. Z.* **329**:232.
SCHOFFA, G. 1964. *Advan. Chem. Phys.* **7**:182.
SOBER, H. A., and E. A. PETERSON. 1960. *In* Amino Acids, Proteins, and Cancer Biochemistry. J. T. Edsall, editor. Academic Press, Inc., New York. 61.
STRYER, L., J. C. KENDREW, and H. C. WATSON. 1964. *J. Mol. Biol.* **8**:46.
THEORELL, H., and A. EHRENBERG. 1951. *Acta Chem. Scand.* **5**:823.
THEORELL, H., and A. EHRENBERG. 1952. *Arch. Biochem. Biophys.* **41**:442.
THEORELL, H., and T. YONETANI. 1964. *Arch. Biochem. Biophys.* **106**:252.
URRY, D. W. 1967. *J. Biol. Chem.* **242**:4441.
WEISS, C., H. KOBAYASHI, and M. GOUTERMAN. 1965. *J. Mol. Spectr.* **16**:415.
WETLAUFER, D. B. 1962. *Advan. Protein Chem.* **17**:303.